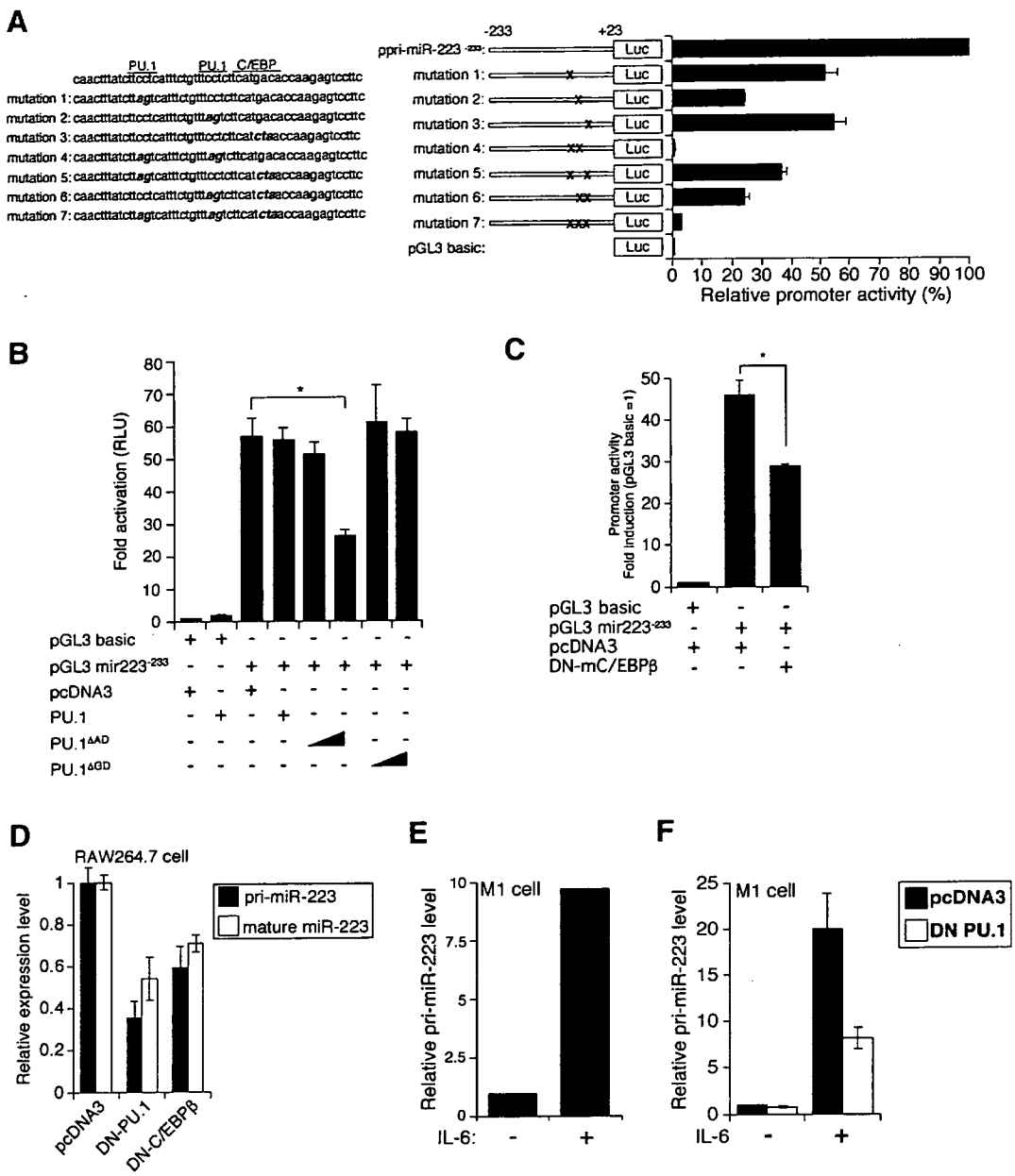

Figure 3. PU.1 as Well as C/EBP as a Regulator of Pri-miR-223 Transcription

(A) The mutant sequences of mouse pri-miR-223 promoter reporter vector are shown (left). The effects of mutations on endogenous pri-miR-223 promoter activity were examined by a luciferase reporter assay. Data are shown as promoter activity relative to the basal endogenous pri-miR-223 promoter activity.

(B and C) Repression of the endogenous mouse pri-miR-223 promoter activity by overexpression of dominant-negative PU.1 (DN-PU.1; B) or C/EBPβ (C). Together with reporter vectors (FL: 0.2 μg, RL; 0.05 μg), indicated expression vectors (0.5 μg) were transfected into RAW264.7 cells. The activity of mouse pri-miR-223 promoter was then examined by a luciferase reporter assay. For DN-PU.1 expression, each expression vector was used with two doses (1[0.5μg] or 1/10). Data are represented as mean ± SD from triplicate assays. * indicates $p < 0.05$ in a Student's t test.

(D) The levels of pri-miR-223 and mature miR-223 in RAW264.7 cells transfected with either pcDNA3, DN-PU.1 ($PU.1^{\Delta AD}$), or DN-C/EBPβ were examined by quantitative real-time RT-PCR as detailed in the Experimental Procedures. Transfectants were enriched as described in the Supplemental Data. Data are shown as mean ± SD from triplicate measurements.

(E) The level of pri-miR-223 in undifferentiated and differentiated M1 cells was examined by quantitative real-time RT-PCR. Data are shown as mean of triplicate assays.

(F) Stable transfectants of M1 cells with either control (pcDNA3) or DN-PU.1 ($PU.1^{\Delta AD}$) expression vector were prepared as described in the Supplemental Data and were cultured in the presence of mrIL-6 for 4 days to induce differentiation. The level of pri-miR-223 in each transfectant was then examined by quantitative RT-PCR. Data are represented as mean ± SD from triplicate tests.

In addition to the assays with DN-PU.1, effects of dominant-negative C/EBPβ (DN-C/EBPβ) expression on the pri-miR-223 promoter activity were also examined, and reduction of the promoter activity was observed as well, confirming a significant role of C/EBPs in activation of the pri-miR-223 promoter (Figure 3C).

Consistent with the roles of PU.1 and C/EBPβ in pri-miR-223 promoter activation, endogenous levels of pri- and mature miR-223 were significantly downregulated by the expression of DN-PU.1 ($PU.1^{\Delta AD}$) or DN-C/EBPβ in RAW264.7 cells (Figure 3D).

Regulation of pri-miR-223 by PU.1 further implicates that the inducible level of miR-223 expression would be synchronous with myeloid differentiation. Indeed, we observed significant upregulation of pri-miR-223 level in M1 cells along with IL-6-induced differentiation into macrophage-like cells (Figure 3E). Consistent with the above results, PU.1 appeared as a critical regulator also for differentiation-induced pri-miR-223 upregulation in M1 cells. The M1-$PU.1^{\Delta AD}$ line that is stably transfected with $PU.1^{\Delta AD}$ vector demonstrated a significantly lower level of pri-miR-223 than that in the M1-mock line after IL-6-induced differentiation (Figure 3F); this also indicates a significant role of PU.1 in pri-miR-223 regulation during myeloid differentiation.

Taken together, our observations indicated that hematopoietic transcription factor PU.1 as well as C/EBPβ are key transcription factors for pri-miR-223 transcription and, therefore, for miR-223 expression.

Regulation of Human miR-223

Given the mechanism for miR-223 expression in the mouse system, we realized a difference between our results and the previous work reporting the mechanism of human miR-223 regulation (Fazi et al., 2005). Hence, we sought to re-examine human miR-223 regulation.

We first searched for the candidate transcript of human pri-miR-223 and found one registered transcript, LOC389865 RNA (XM_374329), which encodes human pre-miR-223 sequence (Figure 4A). This transcript is actually expressed in human bone marrow as detected by RT-PCR (Figure 4A). We then cloned the transcript, and two alternative splicing forms were obtained (Figure 4B). A genome plot of these transcripts demonstrated that this gene has a conventional exon-intron structure as observed in the mouse *miR-223* gene (Figure 4B).

As LOC389865 may not be full-length transcript, we next performed rapid amplification of cDNA ends (RACE) to obtain the information from its 5′ end. This assay would also be informative in discovering whether other alternative transcripts are present or not. We obtained two distinct 5′ RACE products and estimated the consistent lengths for the scales from two alternative splicing forms of human pri-miR-223 (Figure 4C). We then sequenced a total of 36 clones of the RACE products, and 34 clones indicated the exact same transcription start site; also, the other two clones pointed to two sites that are near the major transcription start site (Figure 4D, lower panel).

The region proximal to the transcription start sites of human pri-miR-223 is that genomic region that is highly conserved among different species and is actually homologous to the core promoter of mouse pri-miR-223 (Figure 4D). A reporter assay similar to one in Figure 1C revealed that the 5′-flanking genomic region of cloned human pri-miR-223 has a potent promoter activity in human monocytic leukemia cell lines, THP-1 and U-937, both of which express a substantial level of miR-223 (Figure 4E). Moreover, the deletion of the conserved region completely abolished the promoter activity, showing the promoter structure similar to that of mouse pri-miR-223 (Figure 4E).

Together, our results strongly indicate that, under physiological condition, human miR-223 is probably regulated by the conserved promoter identified in our study as observed in the mouse *miR-223* gene.

Regulation of miR-223 in Acute Promyelocytic Leukemia Cells

We then sought to reassess the regulation of miR-223 in the exactly same experimental system adopted in the previous work (Fazi et al., 2005).

We first determined the transcription start sites of pri-miR-223 in both nontreated and ATRA-treated NB4 cells. Two relatively abundant RACE products (RP1 and RP2) and one minor product (RP3) were obtained in ATRA-treated NB4 cells (Figure 5A). In addition to these products, another minor RACE product (RP4) was detected in nontreated NB4 cells (Figure 5A). Cloning and sequencing of the RACE products revealed that transcripts represented by RP1, RP2, and RP4 are all generated from the exact same major transcription start site identified in the bone marrow sample (Figure 5A, lower panel). The RP4 is the other splicing variant of human pri-miR-223, which was undetectable in either bone marrow or ATRA-treated NB4 cells. The minor product, RP3, was undetectable in bone marrow RNA, and this revealed one alternative transcription start site at 2039 bp downstream of the major transcription start site (Figure 5A, lower panel). Despite the presence of this minor transcription start site, we were convinced that pri-miR-223 in NB4 cells is mainly transcribed from the exact same major transcription start site identified in human bone marrow. Although it is reported that some pri-miRNAs are hardly detectable due to Drosha activity (Lee et al., 2004), this is not the case for pri-miR-223 since the repertoire of pri-miR-223 transcripts in NB4 cells is not altered even by siRNA-mediated Drosha knockdown (Figure S4A).

Using a specific primer set detecting only the major pri-miR-223 transcripts (Figure 5B, middle), we found that the major variants were upregulated in NB4 cells upon ATRA treatment and that this increase of pri-miR-223 was correlated with the upregulation of mature miR-223 (Figure 5B, lower panel). Strikingly, the promoter containing the conserved genomic region was highly activated in NB4 cells during ATRA-induced differentiation (Figure 5C), consistent with the upregulation of pri-miR-223

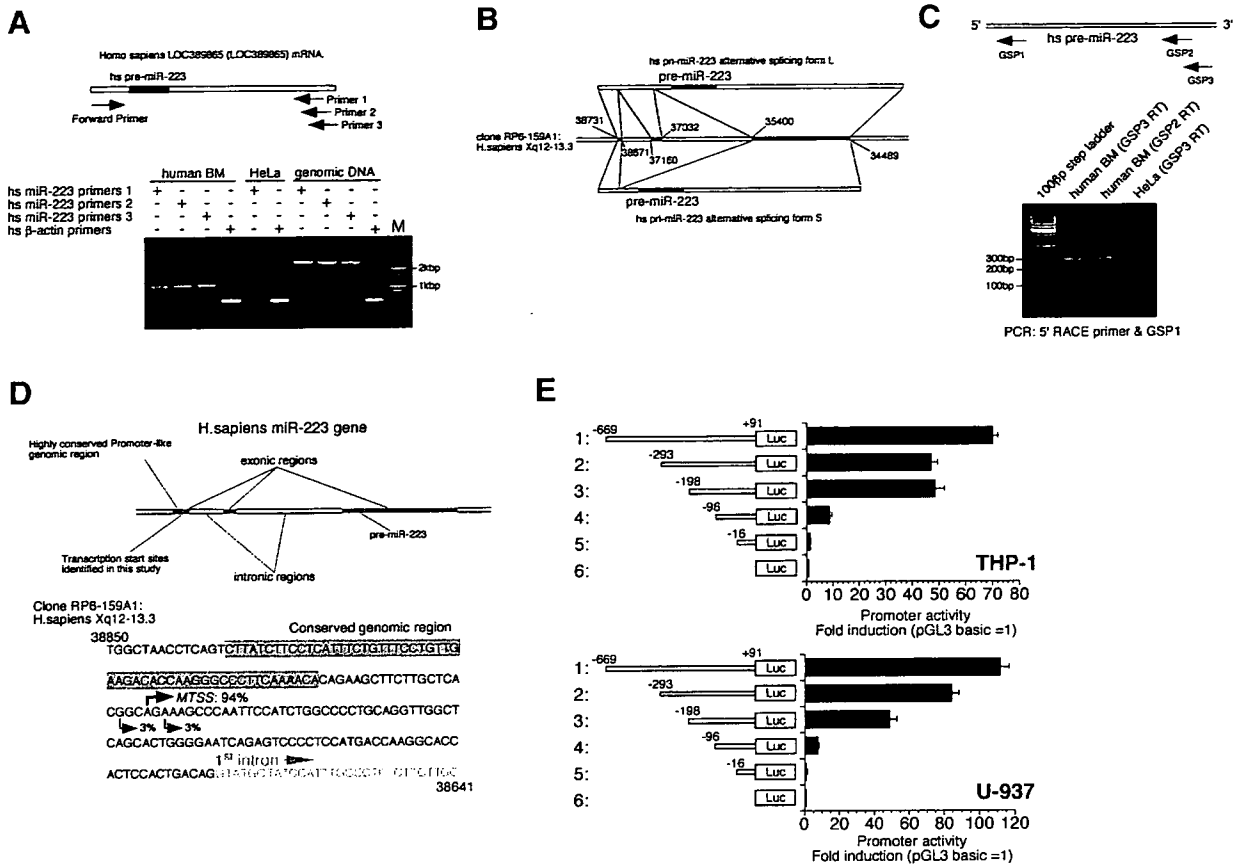

Figure 4. Cloning and Characterization of Human Pri-miR-223 in Bone Marrow

(A) Detection of the putative human pri-miR-223, LOC389865 mRNA, in bone marrow cDNA by RT-PCR with indicated primers.

(B) Cloning of human pri-miR-223. Two alternative splicing forms (Long, L, and Short, S) were cloned as human pri-miR-223, and their genome plots are shown. Numbers denote the position at *H. sapiens* genomic clone, RP6-159A1 from Xq12-13.3.

(C) Cloning of full-length 5′ ends of human pri-miR-223. Full-length transcripts were purified from bone marrow total RNA or HeLa cells and were reverse transcribed with GSP3 to obtain full-length human pri-miR-223 5′ ends.

(D) Schematic for positions of the conserved genomic region, identified transcription start sites, and pre-miR-223 sequence (upper panel). Details of sequences around the transcription start sites of human pri-miR-223 are shown (lower panel). Shaded region indicates the conserved site as shown in Figure 1D and contains the core promoter region. Faint letters denote the first intronic sequence of human pri-miR-223. MTSS indicates *m*ajor *t*ranscription *s*tart *s*ite. Thin arrows indicate the positions of minor transcription start sites.

(E) Luciferase reporter assays were performed in either THP-1 or U937 cells using indicated reporters. 1 indicates ppri-hmiR-223^{-669}-Luc, 2 indicates ppri-hmiR-223^{-293}-Luc, 3 indicates ppri-hmiR-223^{-198}-Luc, 4 indicates ppri-hmiR-223^{-96}-Luc, 5 indicates ppri-hmiR-223^{-16}-Luc, and 6 indicates pGL3 basic.

and the resultant mature miR-223 level in NB4 cells by ATRA treatment.

The roles of PU.1 and C/EBPα in the ATRA-induced pri-miR-223 promoter activity were also examined using RNAi against these molecules. Knockdown of PU.1 resulted in a significant reduction of basal and ATRA-induced pri-miR-223 promoter activity (Figure 5D). The ATRA-inducible pri-miR-223 promoter activity was slightly reduced by a siRNA against C/EBPα (Figure 5D). Consistently, the endogenous level of pri-miR-223 in ATRA-treated NB4 cells was significantly repressed by knockdown of PU.1 using shRNA expression-vector-based RNAi (Figures 5E and 5F). Again, RNAi against C/EBPα resulted in only a slight reduction of ATRA-induced pri-miR-223 upregulation (Figures 5E and 5F). The levels of mature miR-223 were also assayed at the same time and found to be consistent with the levels of pri-miR-223 (Figure S4B). Weak effects of C/EBPα knockdown in the above assays are probably due to redundant activities of other inducible C/EBP members such as C/EBPβ (K.K. and T.F., unpublished data; Duprez et al. 2003) during ATRA-induced differentiation of NB4 cells. Indeed, we observed more effective reduction of the promoter activity and endogenous level of pri-miR-223 in ATRA-treated NB4 cells transfected with DN-C/EBPβ that would suppress actions of multiple C/EBPs (Figures S4C and S4D).

With these results taken together, we concluded that the conserved genomic region acts as pri-miR-223 promoter

in steady state and during ATRA-induced differentiation of NB4 cells and is probably driven by PU.1 and C/EBPs as observed in the mouse miR-223 regulation.

DISCUSSION

Lineage specificity of miR-223 expression is strict as it is detected exclusively in the myeloid compartment of the hematopoietic system (Chen et al., 2004; Figure S2). In this study, we concluded that myeloid expression of miR-223 might be specified by the conserved 5′ proximal *cis*-regulatory element that the myeloid transcription factors, PU.1 and C/EBP, cooperatively act on. In myeloid lineage, there is no single master transcription factor that alone governs myeloid differentiation as seen with Pax5 in B lymphopoiesis (Sieweke and Graf, 1998; Friedman, 2002; Zhu and Emerson, 2002; Rosmarin et al., 2005). Instead, multiple transcription factors work cooperatively and coordinately to control myeloid gene expression (Sieweke and Graf, 1998; Friedman, 2002; Rosmarin et al., 2005; Tenen et al., 1997). Although more than a dozen transcription factors are known to play critical roles in myeloid gene expression (Sieweke and Graf, 1998; Friedman, 2002; Rosmarin et al., 2005), PU.1 and C/EBPs are particularly important as they regulate numerous myeloid genes and are specifically required for myeloid differentiation (Sieweke and Graf, 1998; Friedman, 2002; Rosmarin et al., 2005; Tenen et al., 1997). In this view, together with its myeloid-specific expression, *miR-223* would now be categorized as a member of the so-called "myeloid genes." Neither PU.1 nor C/EBP is truly myeloid restricted since PU.1 is also found in B cells, and C/EBPs are expressed in multiple organs such as liver and adipocytes (Rosmarin et al., 2005). Therefore, myeloid-specific expression of miR-223 probably requires both of these transcription factors. In the presence of a substantial amount of PU.1, C/EBPβ could activate the core promoter in a dose-dependent manner (Figure 2C), indicating that both PU.1 and C/EBP are required for the proper activation of the pri-miR-223 promoter. Together, we speculate that high-level PU.1 confers stable inducibility of the pri-miR-223 promoter activity, and the C/EBP level determines magnitude of the promoter activation in myeloid cells. This idea is consistent with the notion that miR-223 is upregulated during the myeloid differentiation that is associated with increase of PU.1 and C/EBP levels. In addition, we observed repression of endogenous activity of pri-miR-223 promoter by overexpression of erythroid transcription factor, GATA-1 (Figure 2D). This indicates a critical regulatory role of the conserved element in determining pri-miR-223 expression at the turning point of lineage choice between myeloid and erythroid fates, showing an analogy to the regulation of other myeloid genes (Sieweke and Graf, 1998).

Through careful molecular analyses, our study contradicts some aspects of a previous study (Fazi et al., 2005). The miR-223 is evolutionarily conserved, and its expression pattern during myeloid differentiation is also similar in human and mouse systems. However, we did not find the unique C/EBPα-binding element that overlaps with NFI-A-binding site in mouse *miR-223* gene, suggesting that the previously proposed machinery reported in human miR-223 regulation might not be a conserved mechanism of miR-223 regulation. In general, critical genomic elements regulating gene transcription have been conserved during evolution. Furthermore, it has been proposed that the essential genomic elements of miRNAs, including the precursor sequences, might be evolutionary conserved (Berezikov et al., 2005).

Fazi et al. (2005) performed most of their experiments based on the assumption that the unique element for C/EBPα and NFI-A lies in the promoter that they identified for the human miR-223. However, the transcription start sites of human pri-miR-223 that we identified in this study indicated a distinct promoter site. Major transcription start sites are found in a genomic region at a rather large distance from the pre-miR-223 sequence. This region is adjacent to the core promoter of pri-miR-223, which was initially found to be the genomic region highly conserved among different species, including human, mouse, rat, and dog. According to our study, the unique element for C/EBPα and NFI-A competition actually lies in the second intronic region. Therefore, it was still thought to be possible that the element would act as an intronic regulatory element such as an intronic enhancer or repressor. In many cases, intronic regulatory elements are also evolutionarily conserved (Himes et al., 2001). However, there are a few exceptional cases reporting nonconserved intronic enhancers such as in the human adiponectin gene (Qiao et al., 2005). However, even this possibility is unlikely since we could not observe any effects of the intronic sequence on the activity of actual promoter we defined (Figure S4E). Therefore, the actual role of the intronic domain should be revisited in future investigations.

We believe that our study clearly demonstrated the importance of gaining information on pri-miRNAs and neighboring genomic elements for studying miRNA expression. In this view, our approach of finding cDNAs encoding miRNA precursors and following genomic profiling was successful and demonstrated that previously established databases are rich sources of primary miRNA transcripts. Because the databases, like FANTOM3, can provide some information on the tissue origin of each cDNA collection (Yamanaka et al., 2001; Okazaki et al., 2002) in association with EST databases, for example, we can estimate tissue-expression patterns of desired miRNAs by tracing distribution atlases of pairing cDNAs. Indeed, in this study, we could confirm this idea and found an overlapping tissue-expression pattern of miR-223 and its primary transcript, AK036748 (Table 1; Figure S2). In the FANTOM3 database, cDNAs were cloned using the Cap-trapper method that accumulates mRNAs with Cap structure, generating a trustworthy full-length cDNA library (Carninci et al., 2000; Carninci and Hayashizaki, 1999). Determining the exact transcription start sites is a necessary process for analyzing transcriptional regulation of pri-miRNAs,

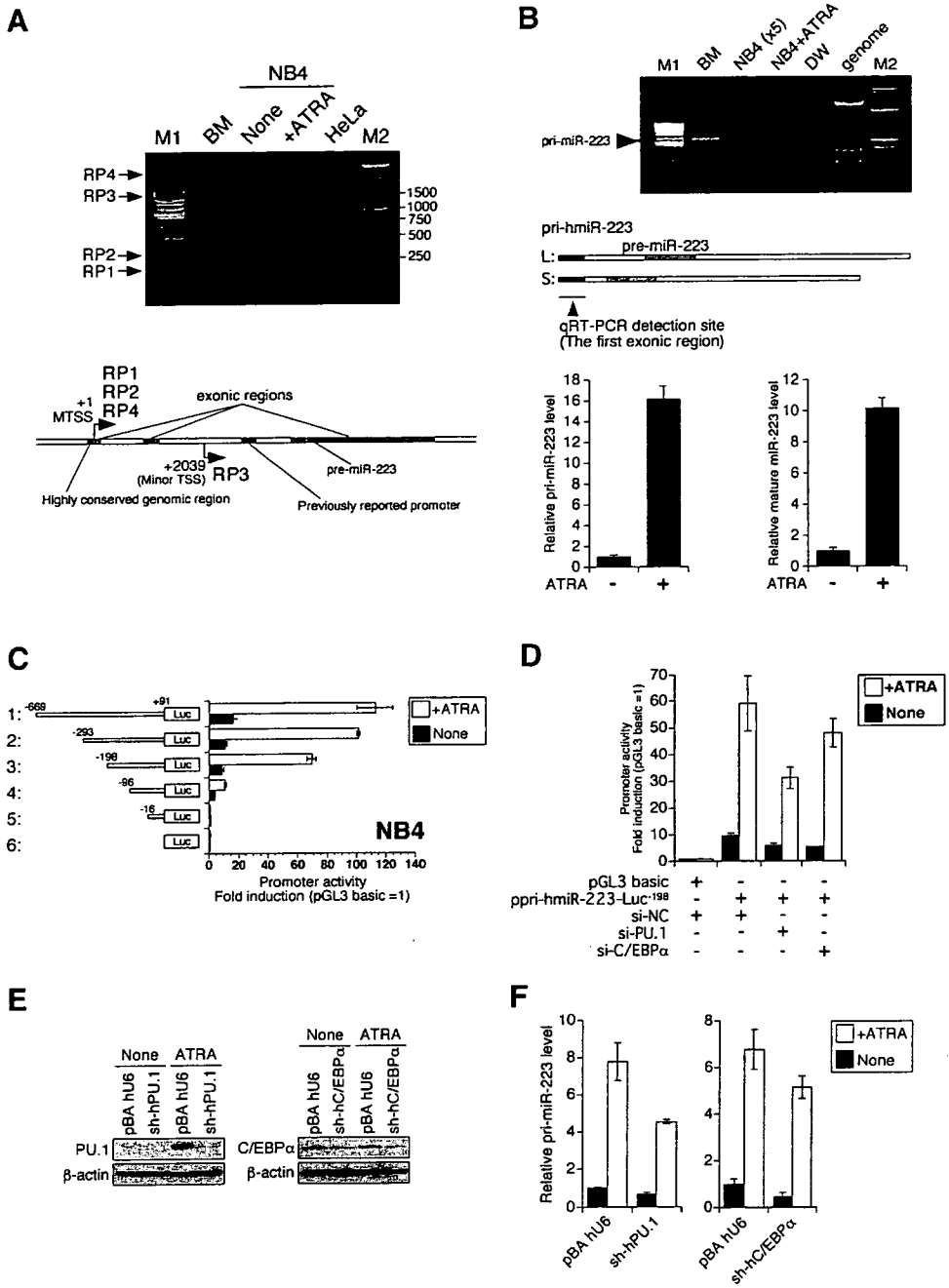

Figure 5. miR-223 Regulation during ATRA-Induced Differentiation of NB4 Cells

(A) Transcription start sites of pri-miR-223 in NB4 cells were determined by 5′ RACE. The 5′ RACE products (RPs) from total RNA samples of bone marrow (BM), NB4 cells (None), ATRA-treated NB4 cells, and HeLa cells are shown (upper panel). M1 indicates 100 bp step ladder; M2 indicates 1 kb DNA ladder (G5711, Promega). The transcription start sites indicated by the 5′ RACE products are shown (lower panel).

(B) Detection of the human pri-miR-223, LOC389865 mRNA, in ATRA-treated and non-treated NB4 cells using PCR with primer set 3 as indicated in Figure 4A (upper panel). BM indicates bone marrow; ×5 indicates five times more RNA template; and DW indicates distilled water. M1 indicates 100 bp step ladder; M2 indicates 1 kb DNA ladder (G5711, Promega). (Middle panel) The target site of human pri-miR-223 for a specific primer set for real-time PCR is shown. (Lower panel) Upregulation of pri-miR-223 (left) and mature miR-223 (right) during ATRA-induced differentiation of NB4 was observed by quantitative real-time PCR.

(C) Potent activation of the conserved pri-hmiR-223 promoter in NB4 cells during ATRA-induced differentiation. Luciferase reporter assay was performed as described in Experimental Procedures. 1 indicates ppri-hmiR-223^{-669}-Luc, 2 indicates ppri-hmiR-223^{-293}-Luc, 3 indicates ppri-hmiR-223^{-198}-Luc, 4 indicates ppri-hmiR-223^{-96}-Luc, 5 indicates ppri-hmiR-223^{-16}-Luc, and 6 indicates pGL3 basic. Data are shown as mean ± SD of triplicate measurements.

and, therefore, our strategy of adopting FANTOM3 was feasible and allowed us to perform a genomic analysis by searching the highly conserved genomic region proximal to the transcription start sites. Such conserved regions were supposed to be critical *cis*-regulatory elements that are actually gene promoters. Here, we could demonstrate that this genome-based analysis lead to the identification of a highly conserved genomic region proximal to the pri-miR-223 transcription start sites that is the actual core promoter and most likely determines myeloid-specific expression of this miRNA. Further, we could identify PU.1 and C/EBP transcription factor-binding motifs, suggesting our approach might prove useful for studying the regulation of other miRNAs. Because gene-expression pattern is regulated by the unique combination of tissue-specific transcription factors, knowing that a specific set of transcription factors binds to a conserved genomic element would give clues for the tissue- and/or cellular-expression pattern of a specific miRNA. Our strategy would also be prominent in this view since many miRNAs have not yet been precisely characterized for their expression patterns and regulatory mechanisms.

Upon the homology search for cDNAs encoding pre-miRNAs, we identified a total of 42 complete pairings of cDNA-pre-miRNAs and practically complete pairings for 33 miRNAs. Further screening for miRNAs with highly conserved genomic regions around the transcription start sites resulted in the identification of ten miRNAs that fit the criterion. Since hundreds of miRNAs have been cloned to date (Bartel and Chen, 2004; Bentwich et al., 2005), this number appears to be very small. However, we should note that cDNAs as putative pri-miRNA candidates presented in this study are for so-called "exonic" miRNAs (Kim and Nam, 2006). There are many miRNAs derived from intronic regions of mRNA-like RNAs that are designated as "intronic" miRNAs (Kim and Nam, 2006). Indeed, a preliminary screening for pri-miRNAs of intronic miRNAs that used a similar approach identified candidate cDNA clones for more than 100 miRNAs (Y.F. and T.F. unpublished data), with many of them bearing conserved genomic elements.

In summary, by exploiting the combination of bioinformatics and biological approaches, we found a transcriptional mechanism for the myeloid expression of mouse miR-223 that is conserved in human miR-223 regulation. Our study thus proposes an evolutionarily conserved mechanism for miR-223 expression, and we propose an alternative to the previous model of Fazi et al. (2005). Further investigation will have to clarify which of the two mechanisms contributes to the regulation of miR-223, whereby the two need not be mutually exclusive.

EXPERIMENTAL PROCEDURES

Bioinformatics

Extraction of mRNA-like RNAs Encoding miRNA Precursor Sequences

A total of 337 precursor sequences of *Mus musculus* miRNA were obtained from the miRBase Sequence Database, Release 8.1 (http://microrna.sanger.ac.uk/sequences/ftp.shtml; Griffiths-Jones, 2004). The Riken FANTOM3 database provides mouse nonredundant, full-length cDNA sequences, and a total 102,802 of those sequences were downloaded (ftp://fantom.gsc.riken.jp/FANTOM3/). A homology search was exhaustively conducted between miRNA precursor sequences and cDNA sequences by using BLAST 2.2.12 with a cutoff value of $E = 1.0e^{-5}$. Among resultant cDNA-pre-miRNA pairs (294 pairs for 61 miRNAs), those with a perfect homology were extracted.

Analyses of Transcription Factor-Binding Sites and Genome Conservation

To identify the transcription start site, cDNA sequences containing pre-miRNA were mapped to the mouse genome, referring to the NCBI database (http://www.ncbi.nlm.nih.gov). Phylogenetic conservation from 250 bp upstream sequence of each 5′ boundary was analyzed in a Mouse BLAT search of the UCSC Genome Browser (http://genome.ucsc.edu/cgi-bin/hgGateway). Putative binding sites for transcription factors of conserved genomic regions were explored by conducting the Transcription Element Search System (http://www.cbil.upenn.edu/tess/index.html).

Cell Culture, Transfection, and DNA Constructs

Conditions of cell cultures and transfections are detailed in the Supplemental Data. Details of plasmid constructions are also described in the Supplemental Data.

Chromatin Immunoprecipitation Assay

ChIP was performed with Chromatin Immunoprecipitation Assay Kit (Upstate Biotechnology, Charlottesville, VA) according to the manufacturer's recommendation. Antibodies used for ChIP were all purchased from Santa Cruz Biotechnology (Santa Cruz, CA). Genomic regions corresponding to promoters of mouse pri-miR-223, Cathepsin C, and c-Myc were amplified by PCR using specific primers shown in Table S1.

Quantitative Real-Time RT-PCR

Total RNA was isolated from cells using mirVana miRNA Isolation Kit (Ambion) or miRNeasy mini kit (Qiagen) with the protocol specialized for total RNA purification. Relative quantification of human pri-miR-223 was performed by real-time PCR with SYBR green I. Level of mouse pri-miR-223 was determined with Taqman technology. Primers amplifying the mouse pre-miR-223 region and a specific Taqman probe were designed with PrimerExpress software (Applied Biosystems). Taqman MicroRNA Assay (Applied Biosystems) technology with a mature miR-223-specific probe and RT and PCR primers were used for quantification of mature miR-223, according to the manufacturer's instructions. Amplification of HPRT mRNA (for pri-miR-223; Applied Biosystems) and U6 small RNA (for mature miR-223; Applied Biosystems) was done with each experimental sample as an endogenous control to account for differences in the amount and quality of total RNA added to each reaction. All primers and the Taqman probe are shown in Table S1.

(D) Effects of synthetic siRNA-mediated PU.1 or C/EBPα knockdown on ATRA-induced pri-miR-223 promoter activity. NC indicates negative control. Data are shown with mean ± SD of triplicate measurements.

(E and F) Knockdown of PU.1 (left) or C/EBPα (p42 isoform; right) by corresponding shRNA vectors was confirmed by western blotting (E). Note that there is significant upregulation of PU.1 upon ATRA-treatment as reported previously (Mueller et al., 2006). A portion of each sample was subjected to measurement of the pri-miR-223 level (F). Transfectants were enriched as described in the Supplemental Data. Data in (F) were shown with mean ± SD of triplicate assays.

RACE

Total RNA from human bone marrow was obtained from Clontech and used for 5′ RACE. For isolation of total RNA from NB4 cells and to avoid any loss of small RNA fractions, we used the mirVana miRNA Isolation Kit or the miRNeasy mini kit (Qiagen) with the protocol specialized for total RNA purification. The 5′ RACE was performed using the GeneRacer kit (Invitrogen). RACE products were obtained by PCR using TaKaRa Ex Taq (TAKARA Bio. Inc., Tokyo, Japan) with the sense primer provided in the GeneRacer kit and the antisense primer specific for human *miR-223* gene listed in Table S1 and were sequenced to determine 5′ ends of human pri-miR-223. For sequencing, RACE products were separated on agarose gels by electrophoresis, and individual bands were cloned using pGEM-T Easy Vector Systems (Promega).

RNA Interference

Knockdown of hPU.1 and hC/EBPα by RNAi was accomplished by transfections of either duplex siRNAs (for the promoter-reporter assay) or shRNA expression vectors. Duplex siRNAs were synthesized by Japan Bio Services Co., LTD. (Saitama, Japan). Both synthetic and vector-based siRNAs target the same sites in corresponding transcription-factor mRNAs, and the sequences are shown in Table S1. The RNAi target sites for hPU.1 and hC/EBPα have been evaluated empirically and literally (Mueller et al., 2006). AllStars Negative Control siRNA was purchased from Qiagen and was used as the negative-control synthetic siRNA.

Western Blotting

Western blotting was performed as described previously (Fukao et al. 2002) and is also detailed in the Supplemental Data. Affinity-purified rabbit anti-PU.1 and -C/EBPα antisera were obtained from Santa Cruz Biotechnology (Santa Cruz, CA). Anti-β-actin antibody was purchased from Sigma.

Supplemental Data

Supplemental Data include Experimental Procedures, References, four figures, and one table and can be found with this article online at http://www.cell.com/cgi/content/full/129/3/617/DC1/.

ACKNOWLEDGMENTS

We would like to thank Drs. Michael Lanotte and Masahiro Kizaki for providing us NB4 cells and Prof. Takatsu and Dr. Takaki for WEHI-231 cells. This work is supported by grants from The Sumitomo Foundation (T.F.), Schering Japan (T.F.), and the Keio Gijuku Fukuzawa Memorial Fund (M.T.).

Received: February 9, 2006
Revised: December 7, 2006
Accepted: February 16, 2007
Published: May 3, 2007

REFERENCES

Bartel, D.P. (2004). MicroRNAs: genomics, biogenesis, mechanism, and function. Cell *116*, 281–297.

Bartel, D.P., and Chen, C.Z. (2004). Micromanagers of gene expression: the potentially widespread influence of metazoan microRNAs. Nat. Rev. Genet. *5*, 396–400.

Bentwich, I., Avniel, A., Karov, Y., Aharonov, R., Gilad, S., Barad, O., Barzilai, A., Einat, P., Einav, U., Meiri, E., et al. (2005). Identification of hundreds of conserved and nonconserved human microRNAs. Nat. Genet. *37*, 766–770.

Berezikov, E., Guryev, V., van de Belt, J., Wienholds, E., Plasterk, R.H., and Cuppen, E. (2005). Phylogenetic shadowing and computational identification of human microRNA genes. Cell *120*, 21–24.

Caminci, P., and Hayashizaki, Y. (1999). High-efficiency full-length cDNA cloning. Methods Enzymol. *303*, 19–44.

Caminci, P., Shibata, Y., Hayatsu, N., Sugahara, Y., Shibata, K., Itoh, M., Konno, H., Okazaki, Y., Muramatsu, M., and Hayashizaki, Y. (2000). Normalization and subtraction of cap-trapper-selected cDNAs to prepare full-length cDNA libraries for rapid discovery of new genes. Genome Res. *10*, 1617–1630.

Caminci, P., Kasukawa, T., Katayama, S., Gough, J., Frith, M.C., Maeda, N., Oyama, R., Ravasi, T., Lenhard, B., and Wells, C. (2005). The transcriptional landscape of the mammalian genome. Science *309*, 1559–1563.

Chen, C.Z., and Lodish, H.F. (2005). MicroRNAs as regulators of mammalian hematopoiesis. Semin. Immunol. *17*, 155–165.

Chen, C.Z., Li, L., Lodish, H.F., and Bartel, D.P. (2004). MicroRNAs modulate hematopoietic lineage differentiation. Science *303*, 83–86.

Duprez, E., Wagner, K., Koch, H., and Tenen, D.G. (2003). C/EBPβ: a major PML-RARA-responsive gene in retinoic acid-induced differentiation of APL cells. EMBO J. *22*, 5806–5816.

Fazi, F., Rosa, A., Fatica, A., Gelmetti, V., De Marchis, M.L., Nervi, C., and Bozzoni, I. (2005). A minicircuitry comprised of microRNA-223 and transcription factors NFI-A and C/EBPα regulates human granulopoiesis. Cell *123*, 819–831.

Friedman, A.D. (2002). Transcriptional regulation of granulocyte and monocyte development. Oncogene *21*, 3377–3390.

Fukao, T., Tanabe, M., Terauchi, Y., Ota, T., Matsuda, S., Asano, T., Kadowaki, T., Takeuchi, T., and Koyasu, S. (2002). PI3K-mediated negative feedback regulation of IL-12 production in DCs. Nat. Immunol. *3*, 875–881.

Griffiths-Jones, S. (2004). The microRNA Registry. Nucleic Acids Res. *32*, D109–D111.

Grove, M., and Plumb, M. (1993). C/EBP, NF-kappa B, and c-Ets family members and transcriptional regulation of the cell-specific and inducible macrophage inflammatory protein 1 alpha immediate-early gene. Mol. Cell. Biol. *13*, 5276–5289.

Himes, S.R., Tagoh, H., Goonetilleke, N., Sasmono, T., Oceandy, D., Clark, R., Bonifer, C., and Hume, D.A. (2001). A highly conserved c-fms gene intronic element controls macrophage-specific and regulated expression. J. Leukoc. Biol. *70*, 812–820.

Katayama, S., Tomaru, Y., Kasukawa, T., Waki, K., Nakanishi, M., Nakamura, M., Nishida, H., Yap, C.C., Suzuki, M., Kawai, J., et al. (2005). Antisense transcription in the mammalian transcriptome. Science *309*, 1564–1566.

Kim, V.N. (2005). MicroRNA biogenesis: coordinated cropping and dicing. Nat. Rev. Mol. Cell Biol. *6*, 376–385.

Kim, V.N., and Nam, J.W. (2006). Genomics of microRNA. Trends Genet. *22*, 165–173.

Lagos-Quintana, M., Rauhut, R., Lendeckel, W., and Tuschl, T. (2001). Identification of novel genes coding for small expressed RNAs. Science *294*, 853–858.

Lau, N.C., Lim, L.P., Weinstein, E.G., and Bartel, D.P. (2001). An abundant class of tiny RNAs with probable regulatory roles in Caenorhabditis elegans. Science *294*, 858–862.

Lee, R.C., and Ambros, V. (2001). An extensive class of small RNAs in Caenorhabditis elegans. Science *294*, 862–864.

Lee, Y., Jeon, K., Lee, J.T., Kim, S., and Kim, V.N. (2002). MicroRNA maturation: stepwise processing and subcellular localization. EMBO J. *21*, 4663–4670.

Lee, Y., Kim, M., Han, J., Yeom, K.H., Lee, S., Baek, S.H., and Kim, V.N. (2004). MicroRNA genes are transcribed by RNA polymerase II. EMBO J. *23*, 4051–4060.

Lipman, D.J. (1997). Making (anti)sense of non-coding sequence conservation. Nucleic Acids Res. *25*, 3580–3583.

Mueller, B.U., Pabst, T., Fos, J., Petkovic, V., Fey, M.F., Asou, N., Buergi, U., and Tenen, D.G. (2006). ATRA resolves the differentiation block in t(15;17) acute myeloid leukemia by restoring PU.1 expression. Blood *107*, 3330–3338.

Nerlov, C., Querfurth, E., Kulessa, H., and Graf, T. (2000). GATA-1 interacts with the myeloid PU.1 transcription factor and represses PU.1-dependent transcription. Blood *95*, 2543–2551.

Okazaki, Y., Furuno, M., Kasukawa, T., Adachi, J., Bono, H., Kondo, S., Nikaido, I., Osato, N., Saito, R., Suzuki, H., et al. (2002). Analysis of the mouse transcriptome based on functional annotation of 60,770 full-length cDNAs. Nature *420*, 563–573.

Orkin, S.H., and Zon, L.I. (2002). Hematopoiesis and stem cells: plasticity versus developmental heterogeneity. Nat. Immunol. *3*, 323–328.

Pasquinelli, A.E., Hunter, S., and Bracht, J. (2005). MicroRNAs: a developing story. Curr. Opin. Genet. Dev. *15*, 200–205.

Qiao, L., Maclean, P.S., Schaack, J., Orlicky, D.J., Darimont, C., Pagliassotti, M., Friedman, J.E., and Shao, J. (2005). C/EBPα regulates human adiponectin gene transcription through an intronic enhancer. Diabetes *54*, 1744–1754.

Rosmarin, A.G., Yang, Z., and Resendes, K.K. (2005). Transcriptional regulation in myelopoiesis: Hematopoietic fate choice, myeloid differentiation, and leukemogenesis. Exp. Hematol. *33*, 131–143.

Sieweke, M.H., and Graf, T. (1998). A transcription factor party during blood cell differentiation. Curr. Opin. Genet. Dev. *8*, 545–551.

Tenen, D.G., Hromas, R., Licht, J.D., and Zhang, D.E. (1997). Transcription factors, normal myeloid development, and leukemia. Blood *90*, 489–519.

Venkatesh, B., and Yap, W.H. (2004). Comparative genomics using fugu: a tool for the identification of conserved vertebrate cis-regulatory elements. Bioessays *27*, 100–107.

Yamanaka, I., Kiyosawa, H., Yagi, K., Tomaru, Y., Hasegawa, Y., Nogami, A., Schonbach, C., Gojobori, T., Baldarelli, R., Hill, D.P., et al. (2001). Functional annotation of a full-length mouse cDNA. Nature *409*, 685–690.

Yekta, S., Shih, I.H., and Bartel, D.P. (2004). MicroRNA-directed cleavage of HOXB8 mRNA. Science *304*, 594–596.

Zhu, J., and Emerson, S.G. (2002). Hematopoietic cytokines, transcription factors and lineage commitment. Oncogene *21*, 3295–3313.

研究成果の刊行に関する一覧表
平成19年度　奈良県立医科大学附属病院　感染症センター　古西　満

雑誌

発表者氏名	論文タイトル名	発表誌名	巻号	ページ	出版年
SHIGEKI HOSHINO, BINLIAN SUN, MITSURU KONISHI, MARI SHIMURA, TATSUYA SEGAWA, YOSHIAKI HAGIWARA, YOSHIO KOYANAGI, AIKICHI IWAMOTO, JUN-ICHI MIMAYA, HIROSHI TERUNUMA, SHIGEYUKI KANO, and YUKIHITO ISHIZAKA	Vpr in Plasma of HIV Type 1-Positive Patients Is Correlated with the HIV Type 1 RNA Titers	AIDS RESEARCH AND HUMAN RETROVIRUSES	23	391-397	2007
Kenji Uno, Mitsuru Konishi, Eiichiro Yoshimoto, Kei Kasahara, Kei Mori, Koichi Maeda, Eiwa Ishida, Noboru Konishi, Koichi Murakawa and Keiichi Mikasa	Fatal Cytomegalovirus-Associated Adrenal Insufficiency in an AIDS Patient Receiving Corticosteroid Therapy	INTERNAL MEDICINE	46	617-620	2007
KENJI UNO, MITSURU KONISHI, EIICHIRO YOSHIMOTO, KEI KASAHARA , KEI MORI, KOICHI MAEDA and KEIICHI MIKASA	A CASE OF GYNECOMASTIA ASSOCIATED WITH EFAVIRENZ	THE JOURNAL OF NARA MEDICAL ASSOCIATION	58	141-145	2007
YOSHINARI MORIMOTO, MITSURU KONISHI, YUICHIRO IMAI, KOUTARO INAGAKE, SATORU FUKUTSUJI and TADAAKI KIRITA	Resistant recurrent aphthous stomatitis in an AIDS patient ～Efficacy and problems of long-term corticosteroid therapy～	Oral Therapeutics and Pharmacology	26	55-59	2007
澤口博千代、中島宏和、中島重徳、古西　満	間質性肺炎発症から後天性免疫不全症候群と判明した２症例	感染症学雑誌	81	67-71	2007

AIDS RESEARCH AND HUMAN RETROVIRUSES
Volume 23, Number 3, 2007, pp. 391–397
© Mary Ann Liebert, Inc.
DOI: 10.1089/aid.2006.0124

Vpr in Plasma of HIV Type 1-Positive Patients Is Correlated with the HIV Type 1 RNA Titers

SHIGEKI HOSHINO,[1,2] BINLIAN SUN,[1] MITSURU KONISHI,[3] MARI SHIMURA,[1] TATSUYA SEGAWA,[4] YOSHIAKI HAGIWARA,[4] YOSHIO KOYANAGI,[5] AIKICHI IWAMOTO,[6] JUN-ICHI MIMAYA,[7] HIROSHI TERUNUMA,[8] SHIGEYUKI KANO,[1,2] and YUKIHITO ISHIZAKA[1]

ABSTRACT

Vpr, an accessory gene product of HIV-1, has been reported in the plasma of HIV-1-positive patients, and exogenous Vpr induces the reactivation of viral production from latently infected cells and the apoptosis of T cells *in vitro*. These observations imply that Vpr is important in AIDS development, but the clinical relevance of the findings cannot be evaluated fully because the actual plasma Vpr concentration in HIV-1-positive patients is unknown. Here we generated two monoclonal antibodies against different portions of Vpr and successfully identified Vpr as a 14-kDa protein in HIV-1-positive patients. Semiquantitative analysis using a recombinant Vpr revealed that the concentration of Vpr in patient plasma was ~0.7 nM (10 ng/ml). Cross-sectional analysis of 52 HIV-1-positive patients revealed that the presence of Vpr detected in 20 patients was positively correlated with HIV-1 RNA copy number ($p < 0.03$), but not with the number of $CD4^+$ T cells. This is the first report demonstrating the actual amount of Vpr in HIV-1-positive patients, and the possible linkage of Vpr and viral titers indicates that it is important to continue to carry out the sequential analysis of Vpr, especially in clinical courses of HIV-1-positive patients. The threshold of viral titers, where Vpr appears in the patients' plasma, if present, contributes to better understanding the role of Vpr in AIDS pathogenesis.

THE ADOPTION OF ANTIRETROVIRAL THERAPY (ART) has improved the prognosis of HIV-1-positive patients.[1] However, the complete elimination of the virus from patients receiving ART is estimated to take more than 60 years.[2] One factor that may be responsible for this problem is that HIV-1 infects macrophages, latent viral reservoirs[3] from which recurrent viral production is induced by various factors.[4] *Vpr*, an accessory gene of HIV-1, encodes a virion-associated 14-kDa protein that may be critical for the primary infection of macrophages.[5–7] Vpr also induces the reactivation of viral reproduction from latently infected cells. The presence of Vpr in the sera of HIV-1-positive patients, along with the induction of viral reproduction by exogenous Vpr,[8,9] implies that Vpr is actively involved in AIDS development. However, it is necessary to determine the concentration of Vpr in patient plasma samples to correctly evaluate the clinical significance of data obtained from *in vitro* experiments. In the current study, we successfully detected Vpr in patients' samples.

The protocol of this study was approved by the ethics committees of the International Medical Centre of Japan, Nara Medical University, Shizuoka Children's Hospital, and five other hospitals in collaboration with Shizuoka Children's Hospital. Blood plasma samples and peripheral blood were obtained from patients who had given informed consent after the experiment was explained to them. Clinical data on 14 outpatients at Nara Medical University, who were enrolled in the initial study, are

[1]Research Institute, International Medical Center of Japan, Shinjuku-ku, Tokyo 162-8655, Japan.
[2]Graduate School of Comprehensive Human Sciences, University of Tsukuba, Tsukuba 305-8577, Japan.
[3]Center for Infectious Diseases, Nara Medical University, Kashihara, Nara 634-8522, Japan.
[4]Immuno-Biological Laboratories, Co., Fujioka, Gunma 375-0005, Japan.
[5]Laboratory of Viral Pathogenesis, Institute for Virus Research, Kyoto University, Sakyou-ku, Kyoto 606-8507, Japan.
[6]Department of Infectious Diseases, The Institute of Medical Science, The University of Tokyo, Minato-ku 108-8639, Tokyo, Japan.
[7]Department of Hematology and Oncology, Children's Hospital of Shizuoka Prefecture, Aoi-ku, Shizuoka 420-8660, Japan.
[8]Biotherapy Institute of Japan, Koutou-ku, Tokyo, 135-0051, Japan.

summarized in Table 1. For the second study, samples from an additional 38 patients were analyzed. The median numbers of HIV-1 RNA copies (32,289.3 copies/ml), $CD4^+$ T cells (449.4 copies/ml), and total white blood cells (5049.0 cells/ml) were determined in all 52 patients. Control healthy plasma samples were obtained from Teragenix Corporation (Kokusai Bio, Tokyo). A recombinant Vpr protein (rVpr) was first prepared as a fusion protein with glutathione *S*-transferase (GST) expressed by pGEX6-P-1, and purified according to the manufacturer's protocol (GE Healthcare Bio-Sciences, Piscataway, NJ). The purified rVpr appeared as a single band on Coomassie brilliant blue staining (supplementary information 1a: SI-1a). Two mouse monoclonal antibodies, 8D1 (IgG2a) and C217 (IgG2b), were generated by immunization with a full-length Vpr peptide, chemically synthesized based on the prototype NL4-3[10] (Osaka Peptide Institute, Osaka), and a synthetic 18-mer amino acid peptide encompassing its carboxy (C)-terminal region (Wako Pure Chemical Industries, Tokyo, Japan), respectively. An enzyme-linked immunosorbent assay (ELISA) was based on 8D1, as the primary antibody, and a purified rabbit IgG antibody, raised against the peptide of the C-terminal 18 amino acids of Vpr (IBL, Fujioka, Japan), as the second antibody. Although the Vpr-ELISA could clearly detect purified rVpr (SI-1b), we found that the system occasionally detected one or more cross-reacting peptide in healthy persons (data not shown). Therefore, we decided to carry out a semiquantitative analysis using immunoprecipitation-Western blotting (IP-WB) analysis, with rVpr quantified by ELISA as the standard. For the IP-WB analysis, 0.5 mg of C217 was bound to Protein G Sepharose (GE Healthcare Bio-Sciences). Each 200 μl of plasma was first treated with DNase I and RNase A for 5 min, and then incubated with 10 μl of C217-coupled beads for 2 h at 4°C. After being washed in buffer with 0.05% Tween-20, the immunoprecipitate was subjected to Western blot analysis. For standard samples, different amounts of purified rVpr were added to 200 μl of control plasma. No detergents were added when the samples were incubated with the primary antibody, so that the IP-WB would detect only soluble Vpr, and not Vpr in viral particles.[10] The detection limit of the system was about 1 ng/ml (0.07 nM) (SI-2a).

Representative results from the IP-WB analysis of 14 plasma samples are shown in Fig. 1a. A definite signal of the 14-kDa protein was observed in patients N-09, 11, and 13 (Fig. 1a). By contrast, no peptides around 14 kDa were detected in more than 60 specimens from healthy volunteers (Fig. 1b). Because the IP-WB could selectively detect the 14-kDa peptide in the culture supernatant of cells containing an expression plasmid encoding *vpr* (SI-2b), we concluded that the 14-kDa peptide detected by the IP–WB was Vper. A comparison of the signal intensities of the detected bands and standard rVpr (Fig. 1a; 5, 2.5, and 1.25 μg/ml signals, and N-11) indicated that the serum Vpr concentration was about 0.7 nM.

During the analysis, we did not detect the Vpr signal in one patient (N-10; Table 1) who had 11,000 copies/ml of HIV-1 RNA (Fig. 1a, lower panel). To evaluate whether our system failed to detect Vpr mutants differing from the prototype NL4-3 (GenBank accession number M19921), we amplified DNA fragments from peripheral blood mononuclear cells covering the entire *vpr* gene. Then we determined its nucleotide sequence (Fig. 2a, and primers in SI-3). The deduced amino acid sequences are also shown in Fig. 2b. Interestingly, the *vpr* gene from patient N-10 had a four-nucleotide (TTAA) insertion at

TABLE 1. CLINICAL DATA OF PATIENTS SUBJECTED TO ANALYSIS AND RESULTS OF THE IP-WB

						Clinical data				
						White blood cells ($/mm^3$)				
Case number	*Sex*	*Age*	*Causes of infection*	*Conditions*	*Treatment status*[a]	*Total number*	*Lymphocytes*	*$CD4^+$ T cells*	*HIV-1 RNA (copies/ml)*	*Vpr*[b]
N-01	M	39	HO[c]	AIDS[d]	2	8400	2612	771	<50	−
02	M	41	HO	AIDS	2	6800	2584	346	<50	−
03	M	59	HE[c]	AIDS	2	4700	2444	381	260	−
04	F	32	HE	AC[d]	3	6300	1890	302	4,400	−
05	M	38	HO	AIDS	2	8600	2417	585	<50	−
06	M	35	HO	AC	1	4900	1274	116	220,000	+++
07	M	45	BL[c]	AIDS	2	2600	546	38	73,000	++
08	M	58	HE	AIDS	2	6800	1632	366	<50	−
09	M	29	BL	AC	1	3000	1056	266	17,000	+
10	M	23	HO	AC	1	5200	1300	230	11,000	−
11	F	37	HE	AC	1	4600	1150	222	500,000	+++
12	F	40	HE	AC	1	6600	1584	598	98	−
13	M	42	BL	AIDS	2	3100	1054	110	70,000	++
14	M	23	HO	AC	1	5800	2656	553	71,000	++

[a]Group 1, no therapy; group 2, under medication; group 3, posttherapy.

[b]Based on results of the IP-WB, patients are divided into four groups; Vpr-negative (−) and Vpr-positive with less than 1 ng/ml (+), with 1–5 ng/ml (++), and with more than 5 ng/ml (+++).

[c]HO, homosexual; HE, heterosexual; BL, blood products.

[d]AIDS, acquired immunodeficiency syndrome; AC, asymptomatic carrier.

nucleotide 81, designated "clone 10," which generates a frameshift mutation within the inserted sequence (shown by the box in Fig. 2a). However, because this patient had no deletion in the 3′ region of the *vpr* gene, it was possible to clone the gene. Repeated sequence analyses of several clones of the amplified *vpr* DNA indicated that clone 10 was the major *vpr* in this patient (Table 2). The negative results of the IP-WB analysis for patient N-10 were therefore due to truncation of the C-terminal region.

Additional sequence analysis revealed that "clone N (Nara)," which differs by four amino acids from the prototype NL4-3 (Fig. 2b), was frequently observed in the analyzed patients (patients N-04, 05, 08, 09, 11, and 12). Interestingly, although patient N-09 had clone N as a major variant—all seven clones sequenced from the PCR products were identified as clone N (see Table 2)—the IP-WB analysis (Fig. 1a, lower panel) detected a positive Vpr signal in patient N-09. This suggests that C217 antibody, which was used as the first antibody in immunoprecipitation, reacts with the protein encoded by clone N, even though its C-terminal region differs from the prototype NL4-3 clone by two amino acids (Fig. 2b).

Next, we examined the possible correlation of Vpr and clinical manifestations. An analysis of 14 patients suggested a positive link between Vpr and viral titers (data not shown). To examine this possibility, we analyzed an additional 38 stocked samples using IP-WB. We detected Vpr in 14 samples. A representative result of the second analysis is shown in Fig. 1c. Positive Vpr signals were detected in patients T-166, 167, and 175. Then we examined the relationship between Vpr and RNA copy number in total 52 samples. As shown in Fig. 3a, we found a positive correlation between the detection of Vpr and RNA copy number ($p < 0.03$). In contrast, we did not detect a positive relationship between Vpr and the numbers of $CD4^+$ T cells or total white blood cells. The distribution of Vpr-positive patients based on the concentration of Vpr implied that the high amount of Vpr is observed in patients with high HIV-1 RNA copy numbers (Fig. 3b).

In the current work, we successfully identified Vpr in 20 samples from 52 HIV-1-positive patients. A comparison of the signals obtained with standard rVpr revealed that the Vpr concentration was ~0.7 nM. Levy *et al.*[9] suggested that Vpr is present in patient plasma, with rVpr activating viral reproduction when added to the culture medium of latently infected cells. In addition, Muthumani *et al.* proposed that exogenous rVpr has various activities, such as inducing T cell apoptosis,[11] inhibiting macrophage function,[12] and suppressing NF-κB signaling.[13] However, these experiments did not consider the actual amount of Vpr present in the plasma samples. Our result is the first demonstration of Vpr in HIV-1-positive patients, and provides a rationale for the dose of rVpr suitable for *in vitro* experiments.

We observed a positive correlation between the detection of Vpr and HIV-1 RNA copy number ($p < 0.03$) (Fig. 3a). It has been reported that the exogenous Vpr induces viral production from latently infected cells, implying that Vpr is involved in viral reproduction *in vivo*. An important question still to be answered is how the Vpr titer changes in the context of viral replication during the clinical course of the disease. It is important to clarify whether Vpr functions as an initial trigger of viral expansion *in vivo*.

We did not detect a link between Vpr and the numbers of $CD4^+$ T cells. Recently, it was determined that WT-Vpr and its variant R77Q act differently in modifying the clinical features of HIV-1-positive patients. Based on several reports, it has been proposed that R77Q is a candidate marker for long-term nonprogression (LTNP),[14–16] although this is still controversial.[17,18] In this study, we observed that the main Vpr variants of patients N-04, 09, and 10 were R77Q or C-terminally truncated. However, we did not recognize these patients as candidates for LTNP (clinical observation by M. Konishi). The involvement of WT-Vpr and R77Q in patients is rationalized by *in vitro* experiments showing that rVpr induces the apoptosis of $CD4^+$ T cells.[11,12,14,15] whereas R77Q has less potent apoptosis activity than WT-Vpr.[15] It is important to note that the *in vitro* studies of the differential activities of exogenous WT-Vpr and R77Q used tremendous amounts of the proteins, and a difference in activity was observed only when 1.5–2.0 μM of the peptides was used.[15] As shown here, the concentration of Vpr in patient plasma was a maximum of 1.0 nM, and it is crucial to compare the functional difference of these molecules at a concentration comparable to that observed *in vivo*. Careful studies are required to address this matter.

SUPPLEMENTARY INFORMATION

SI-1. Purification of rVpr and measurement using ELISA. (**a**) Expression and purification profiles of rVpr. Vpr was expressed as a fusion protein with GST and purified in a glutathione column. Lane 1, marker; lane 2, initial lysate; lane 3, flow-through sample eluted from the glutathione column; lane 4, eluate from rVpr after treatment with precision protease; and lane 5, eluate from an affinity column containing a monoclonal antibody against Vpr (8D1). The arrowhead and arrow indicate the position of GST-Vpr and purified rVpr, respectively. Proteins were stained with Coomassie brilliant blue solution. (**b**) ELISA verion-1 for measuring rVpr. Synthesized full-length Vpr was used to make a standard curve. To the Vpr-ELISA were added 10 ng/ml each of GAPDH, HIV-1 integrase, and SARS-CoV Spike protein, which were expressed as a (His)-tagged protein, and purified using Ni-beads. Note that none of the samples gave cross-signals with Vpr. The amount of rVpr was assessed using the absorbance at OD450 nm, as shown with the dotted line.

SI-2. Detection of Vpr by the IP-WB. (**a**) Sensitivity of the system. The IP-WB analysis was conducted using C217 for IP and 8D1 for WB. To determine the sensitivity of the system, 10, 5, 2.5, and 1.25 ng of purified rVpr were added to 200 μl of plasma from a healthy human just before the IP-WB analysis. The signals obtained using IP-WB (upper panel) and the input rVpr (lower panel) detected by 8D1 are shown. (**b**) Detection of Vpr in a culture supernatant. Culture supernatants (sup.) of 293FS cells (Invitrogen) transfected with pcDNA3.1 (center lane, "Vec") or pcDNA3.1-*vpr* (right lane, "Vpr") were collected on day 6 after transfection, and the IP-WB analysis was carried out. The rVpr (400 pg/lane) was included in the same blot as a positive control of WB (left lane).

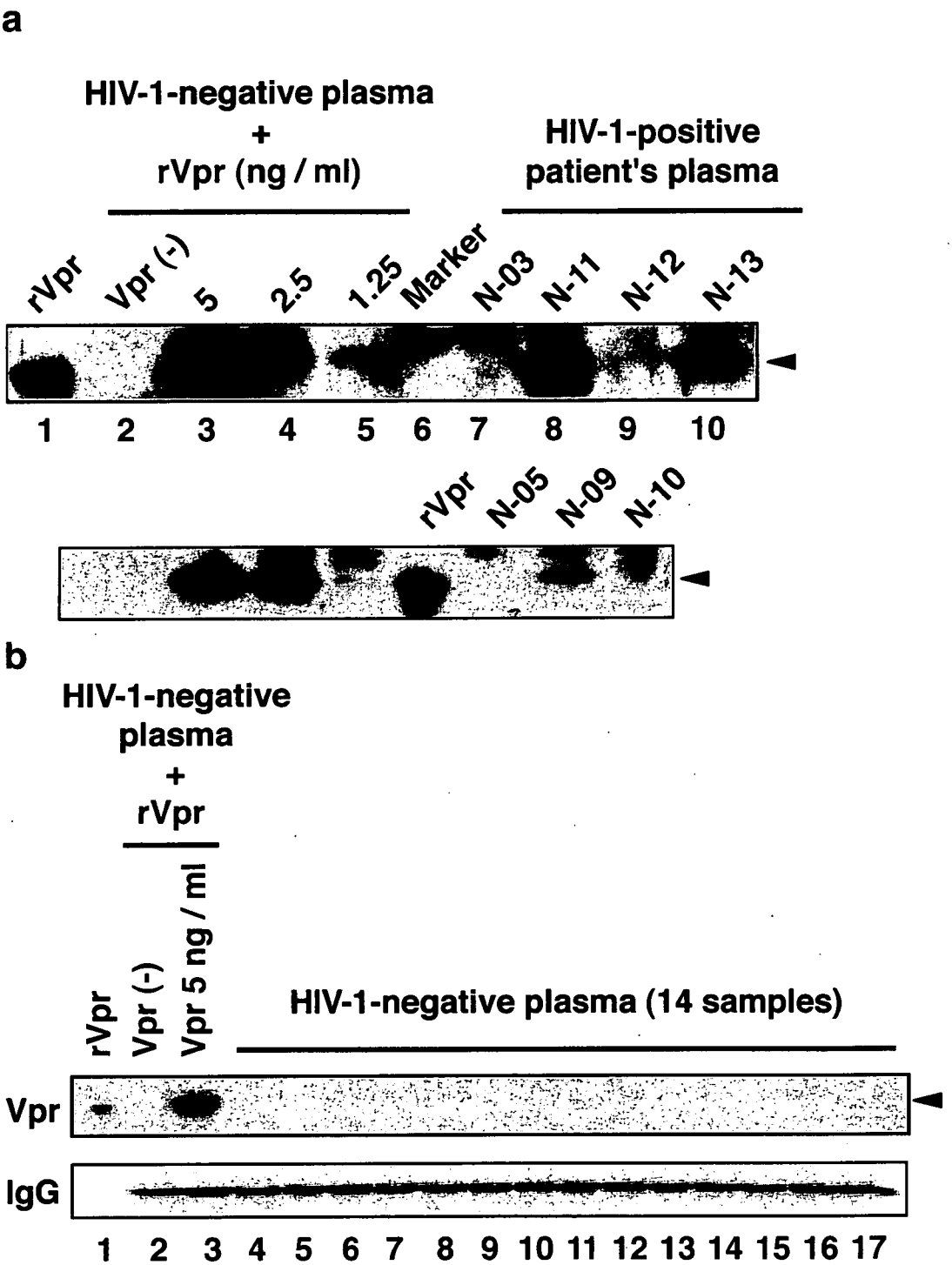

FIG. 1. Detection of Vpr in sera of HIV-1-positive patients. (a) Presence of the 14-kDa Vpr protein in HIV-1-positive patients. To semiquantify the Vpr concentration in patient samples, 5, 2.5, and 1.25 ng of standard rVpr (lanes 2–5), which had been measured using ELISA version-1 (see supplementary information 1b; SI-1b), were included. As a positive control for the WB analysis, 1 ng of rVpr (lane 1) was also included. Signals of HIV-1-positive plasma (lanes 7–10) and a molecular marker (lane 6) are shown. (b) Representative results of the IP-WB analysis of healthy volunteers. The IP-WB analysis was performed on more than 60 samples from healthy volunteers, and representative results from 14 cases (lanes 4–17) are shown. Note that no signals were detected around 14 kDa. The results for input rVpr (lane 1), no rVpr (lane 2), or 5 ng Vpr (lane 3) added to normal plasma are shown. IgG signals recovered after IP are also shown (lower panel). (c) Detection of the 14-kDa Vpr protein in HIV-1-positive patients in the second group. Also in this analysis, 5, 2.5, and 1.25 ng of standard rVpr (lanes 2–5) were included to assess the concentration of Vpr in patient plasma samples.

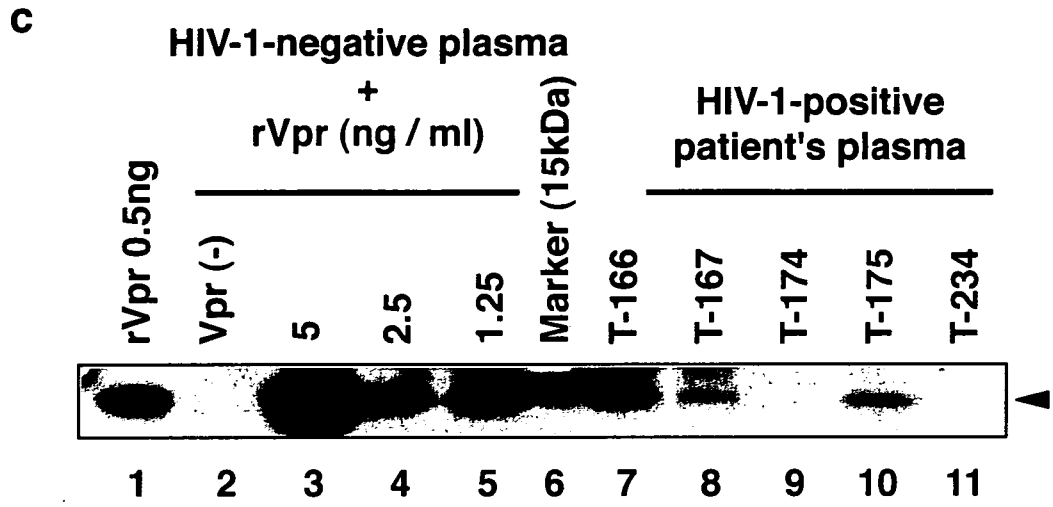

FIG. 1. (*Continued*).

SI-3. Cloning and sequence analysis of *vpr*. DNA covering *vpr* was amplified from the genomic DNA of peripheral blood cells using nested PCR. The primers used were Vpr1F (nt 4713–4733, 5′-GACCCTGACCTAGCAGACCA-3′) and Vpr1R (nt 5298–5318, 5′-CAAACTTGGCAATGAAAGCA-3′) for the first PCR. For the second PCR, Vpr2F (nt. 4854–4875, 5′-CAGTACTTGGCACTAGCAGCA-3′) and Vpr2R (nt 5243–5263, 5′-TAGGCTGACTTCCTGGATGC-3′) were used (GenBank accession number M19921). The first and second rounds of PCR were performed for 30 cycles of 95°C for 30 sec, 62°C for 30 sec, and 72°C for 1 min and for 95°C for 30 sec, 64°C for 30 sec, and 72°C for 45 sec, re-

a

```
NL4-3     1 ATGGAACAAG CCCCAGAAGA CCAAGGGCCA CAGAGGGAGC CATACAATGA ATGGACACTA
Clone-10  1 ---------- ---------- ---------- ---------- ---------- ----------

         61 GAGCTTTTAG AGGAACTTAA     GAGTGA AGCTGTTAGA CATTTTCCTA GGATATGGCT
         61 ---------- ---------- TTAA------ ---------- ---------- ----------

        117 CCATAACTTA GGACAACATA TCTATGAAAC TTACGGGGAT ACTTGGGCAG GAGTGGAAGC
        121 ---------- ---------- ---------- ---------- ---------- ----------

        177 CATAATAAGA ATTCTGCAAC AACTGCTGTT TATCCATTTC AGAATTGGGT GTCGACATAG
        181 ---------- ---------- ---------- ---------- ---------- ----------

        237 CAGAATAGGC GTTACTCGAC AGAGGAGAGC AAGAAATGGA GCCAGTAGAT CCTAG 291nt.
        241 ---------- ---------- ---------- ---------- ---------- ----- 295nt.
```

b

```
NL4-3     MEQAPEDQGPQREPYNEWTLELLEELKSEAVRHFPRIWLHNLGQHIYETYGDTWAGVEAIIRILQQLLFIHFRIGCRHSRIGVTRQRRARNGASRS
Clone-10  ..........................N*
Clone-N   ..................................................................Q.....II............
```

FIG. 2. Sequence analysis of *vprs* and the deduced amino acids of Vpr variants in HIV-1-positive patients. The *vpr* gene was amplified and analyzed, as described in SI-3. (**a**) Nucleotide sequence of clone 10. The nucleotide sequence was compared with that of the prototype NL4-3. Clone 10 has a four-base insertion at nucleotide 81, generating a stop codon within the insert (indicated by the box). Nucleotides that are the same as those in NL4-3 are marked with small bars. (**b**) Amino acid sequences of Vpr variants found in the patients. The amino acids deduced from the obtained sequences and the NL4-3 clone are shown. As described in SI-3a, clone 10 was recognized as a major variant in patient N-10, while clone N was the major variant in patients N-04 and 09.

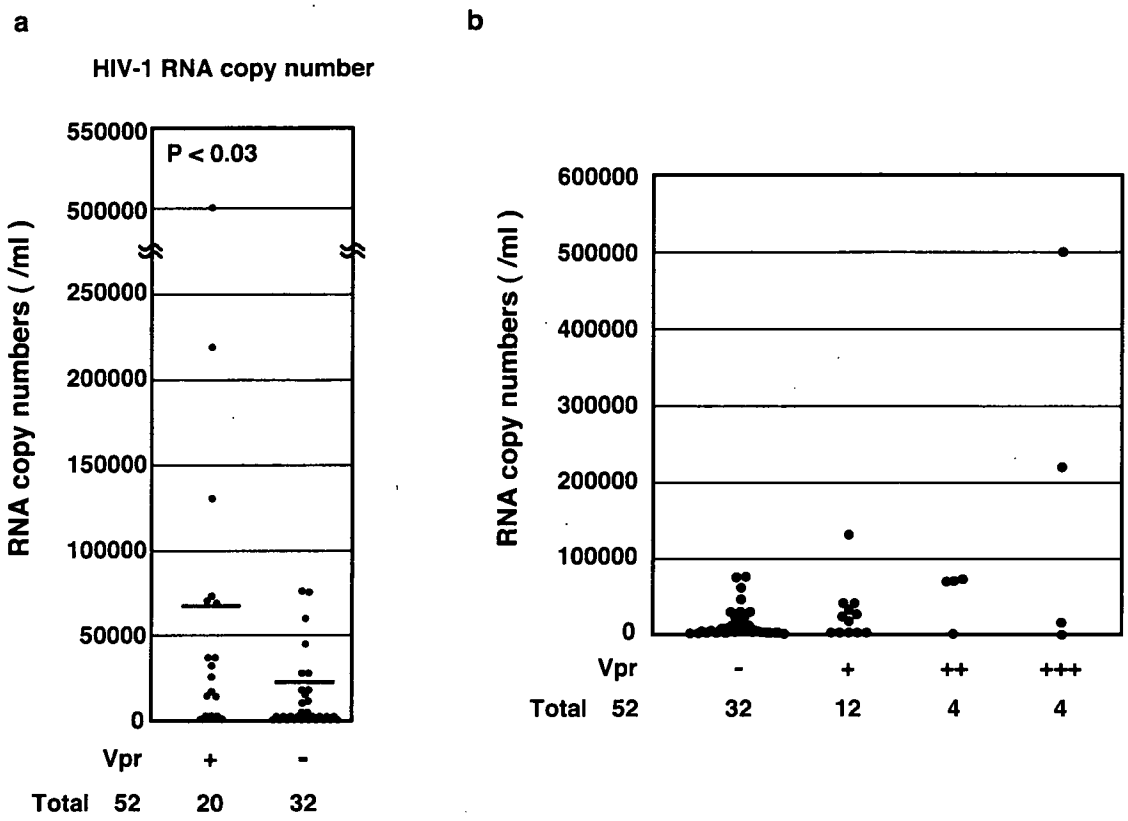

FIG. 3. Correlation between Vpr detection and clinical data. The analyzed cases were divided into Vpr-positive and Vpr-negative groups, and the statistical analysis was done using Student's *t*-test. (**a**). The relationships with the HIV-1 RNA copy number. The bars indicate the mean numbers in each group. The difference for HIV-RNA copy number with Vpr was statistically significant ($p < 0.03$). (**b**) Distribution of Vpr-positive patients according to the concentration of plasma Vpr. Based on the semiquantitative analysis, patients were divided into four groups: Vpr-negative (−), Vpr-positive with less than 1 ng/ml (+), 1–5 ng/ml (++), and more than 5 ng/ml (+++). Each dot means a patient.

spectively. The PCR products were cloned into pZeroBlunt topo vector (Invitrogen, Carlsbad, CA). Several clones were sequenced for each PCR product.

SI-4. See Table 2.

TABLE 2. FREQUENCY OF *vpr* VARIANTS IN HIV-1 PATIENTS[a]

	vpr *variants*		
Cases	*NL4-3*	*Clone N*	*Clone 10*
N-03	7[b]	—	9
N-04	—	14	—
N-05	2	2	3
N-09	—	7	—
N-10	—	—	5
N-12	4	4	—

[a]PCR products amplified from patient genomic DNA were subcloned into the vector, and several clones were sequenced. The numbers in the table indicate the frequency of clones encountered in the sequence analyses. All 5 clones derived from patient N-10 were clone 10. In patients N-04 and 09, clone N was identified as the major variant; all 14 clones for patient N-04 and all 7 clones for patient N-09 were clone N. Patients N-03 and N-05 each had 2 *vpr* variants.

[b]Number of analyzed clones.

ACKNOWLEDGMENTS

We thank the healthy volunteers and C. Nakai-Murakami for donating peripheral blood and providing technical assistance. We are grateful for samples of HIV-1-positive patients to Drs. C. Kobayashi (National Hospital Organization Chiba Medical Center), I. Sato (National Hospital Organization Sendai Medical Center), H. Hanafusa (Ogikubo Hospital), J. Matsuda (Teikyo University School of Medicine), M. Sakai (University of Occupational and Environmental Health), S. Ikeda (Sasebo Municipal Hospital), and T. Fujii (Hiroshima University School of Medicine). This work was supported by a Grant-in-Aid for Research on Health Sciences focusing on Drug Innovation from the Japan Health Sciences Foundation Research and Research on HIV/AIDS from the Ministry of Health, Labor and Welfare of Japan. Dr. Sun is a research resident supported by the Foundation for AIDS prevention.

REFERENCES

1. Palella FJ, Delaney KM, Moorman AC, Loveless MO, Fuhrer J, Satten GA, *et al.*: Declining morbidity and mortality among patients with advanced human immunodeficiency virus infection. N Engl J Med 1998;338:853–860.

2. Finzi D, Hermankova M, Pierson T, Carruth LM, Buck C, Chaisson RE, *et al.*: Identification of a reservoir for HIV-1 in patients on highly active antiretroviral therapy. Science 1997;278:1295–1300.
3. Folks TM, Justement J, Kinter A, Dinarello CA, Fauci AS: Cytokine-induced expression of HIV-1 in a chronically infected promonocyte cell line. Science 1987; 238:800–802.
4. Koyanagi Y, O'Brien WA, Zhao JQ, Golde DW, Gasson JC, and Chen ISY: Cytokines alter production of HIV-1 from primary mononuclear phagocytes. Science 1988;241:1673–1675.
5. Heinzinger NK, Bukrinsky MI, Haggerty SA, Ragland AM, Kewalramani V, Lee MA, *et al.*: The Vpr protein of human immunodeficiency virus type 1 influences nuclear localization of viral nucleic acids in nondividing host cells. Proc Natl Acad Sci USA 1994;91:7311–7315.
6. Vodicka MA, Koepp DM, Silver PA, and Emerman M: HIV-1 vpr interacts with the nuclear transport pathway to promote macrophage infection. Genes Dev 1998;12:175–185.
7. Jenkins Y, McEntee M, Weis K, and Greene WC: Characterization of HIV-1 vpr nuclear import: Analysis of signals and pathways. J Cell Biol 1998;143:875–885.
8. Levy DN, Refaeli Y, MacGregor RR, and Weiner DB: Serum vpr regulates productive infection and latency of human immunodeficiency virus type 1. Proc Natl Acad Sci USA 1994;91:10873–10877.
9. Levy DN, Refaeli Y, and Weiner DB: Extracellular vpr protein increases cellular permissiveness to human immunodeficiency virus replication and reactivates virus from latency. J Virol 1995;69: 1243–1252.
10. Marzio PD, Choe S, Ebright M, Knoblauch R, and Landau NR: Mutational analysis of cell cycle arrest, nuclear localization, and virion packaging of human immunodeficiency virus type 1 vpr. J Virol 1995;69:7909–7916.
11. Muthumani K, Hwang DS, Desai BM, Zhang D, Dayes N, Green DR, *et al.*: HIV-1 vpr induces apoptosis through caspase 9 in T cells and peripheral mononuclear blood cells. J Biol Chem 2002; 277:37820–37831.
12. Muthumani K, Hwang DS, Choo AY, Mayilvahanan S, Dayes NS, Thieu KP, *et al.*: HIV-1 vpr inhibits the maturation and activation of macrophages and dendritic cells *in vitro*. Int Immunol 2004; 17:103–116.
13. Muthumani K, Choo AY, Zong W-X, Madesh M, Hwang DS, Premkumar A, *et al.*: The HIV-1 vpr and glucocorticoid receptor complex is a gain-of-function interaction that prevents the nuclear localization of PARP-1. Nat Cell Biol 2006;8:170–179.
14. Lum JJ, Cohen OJ, Nie Z, Weaver JG, Gomez TS, Yao X-J, *et al.*: *Vpr* R77Q is associated with long-term nonprogressive HIV infection and impaired induction of apoptosis. J Clin Invest 2003; 111:1547–1554.
15. Rodes B, Toro C, Paxinos E, Poveda E, Martinez-Padial M, Benito JM, *et al.*: Differences in disease progression in a cohort of long-term non-progressors after more than 16 years of HIV-1 infection. AIDS 2004;18:1109–1116.
16. Mologni D, Citterio P, Menzaghi B, Zanone PB, Riva C, Broggini V, *et al.*: Vpr and HIV-1 disease progression: R77Q mutation is associated with long term control of HIV-1 infection in different groups of patients. AIDS 2006;20:567–574.
17. Cavert W, Webb CH, Balfour HH Jr: Alterations in the C-terminal region of HIV-1 accessory gene vpr do not confer clinical advantage to subjects receiving nucleoside antiretroviral therapy. J Infect Dis 2004;20:2181–2184.
18. Chui C, Cheung PK, Brumme CJ, Mo T, Brumme ZL, Montaner JSG, *et al.*: HIV-1 VprR77Q mutation does not influence clinical response of individuals initiating highly active antiretroviral therapy. AIDS Res Hum Retrovir 2006;22:615–618.

Address reprint requests to:
Yukihito Ishizaka
Research Institute
International Medical Center of Japan
1-21-1 Toyama
Shinjuku-ku
Tokyo 162-8655, Japan

E-mail: zakay@ri.imcj.go.jp

INTERNAL MEDICINE

□ CASE REPORT □

Fatal Cytomegalovirus-Associated Adrenal Insufficiency in an AIDS Patient Receiving Corticosteroid Therapy

Kenji Uno[1], Mitsuru Konishi[1], Eiichiro Yoshimoto[1], Kei Kasahara[1], Kei Mori[1], Koichi Maeda[2], Eiwa Ishida[3], Noboru Konishi[3], Koichi Murakawa[4] and Keiichi Mikasa[1]

Abstract

A 35-year-old homosexual man, who had already received sulfamethoxazole/trimethoprim and steroid therapy because of human immunodeficiency virus (HIV)-related *Pneumocystis jiroveci* pneumonia, was referred to our hospital. He was also diagnosed as having cytomegalovirus (CMV) co-infection, and started receiving intravenous gancyclovir for CMV infection on the 2nd day of admission into our hospital. He had to continue the steroid therapy because his respiratory condition did not improve. On the 10th hospitalization day, when 40 mg of prednisolone was administered, cardiopulmonary arrest suddenly occurred, and his laboratory data showed hyponatremia and hyperpotassemia. In spite of resuscitation, he died two days later. The postmortem examination revealed that he died of adrenal failure due to CMV infection. In general, CMV is thought to cause adrenalitis, but rarely leads to manifestations of adrenal insufficiency during the clinical course. It is important to be aware that grave adrenal failure due to CMV infection can develop even under steroid therapy.

Key words: AIDS, cytomegalovirus, adrenal insufficiency, corticosteroid

(DOI: 10.2169/internalmedicine.46.1886)

Introduction

Recent advances in antiretroviral therapies have dramatically decreased the mortality rate of acquired immunodeficiency syndrome (AIDS). Despite these advances, opportunistic infections still develop, particularly in the patients who already have severe immunosuppression following the diagnosis of HIV infection. Predilection of cytomegalovirus (CMV) to the adrenal gland has been recognized, and many autopsy studies have revealed CMV invasion to the adrenal gland in AIDS patients. However, clinical adrenal insufficiency rarely develops in HIV-infected patients. We herein report an AIDS patient who died of CMV-induced adrenal failure detected on autopsy examination.

Case Report

A 35-year-old homosexual man had non-productive cough, fever, and exertional dyspnea since May 2004. He went to a neighborhood hospital 12 days before admission into our hospital. He was given azithromycin, but his symptoms did not improve, and he was admitted into the hospital 10 days before he was referred to our hospital because his chest radiography revealed a diffuse interstitial infiltrate. At the previous hospital, 1,000 mg of pazufloxacin was administered, but his respiratory condition became worse. Seven days before admission into our hospital, steroid pulse therapy (1 g/day) was administered for 3 days because of severe hypoxemia. His plasma β-D-glucan was 271 pg/ml 6 days before admission, and 12 tablets of sulfamethoxazole (4.8 g)/trimethoprim (960 mg) and 50 mg of itraconazole were administered 4 days before admission. He was referred to our hospital on June 25 because his serum HIV-1 antibody was positive (Fig. 1).

On admission, his blood pressure was 86/54 mmHg, and his respiratory rate was 30/min. Fine crackles were heard over his bilateral lower lung fields, and hepatomegaly was detected by palpation.

Laboratory data on admission showed anemia, hypoalbu-

[1] Center for Infectious Diseases, Nara Medical University, Nara, [2] Department of General Medicine, Nara Medical University, Nara, [3] Department of Pathology, Nara Medical University, Nara and [4] Sekiya Hospital, Nara
Received for publication May 18, 2006; Accepted for publication January 25, 2007
Correspondence to Dr. Kenji Uno, ukenji@naramed-u.ac.jp

DOI: 10.2169/internalmedicine.46.1886

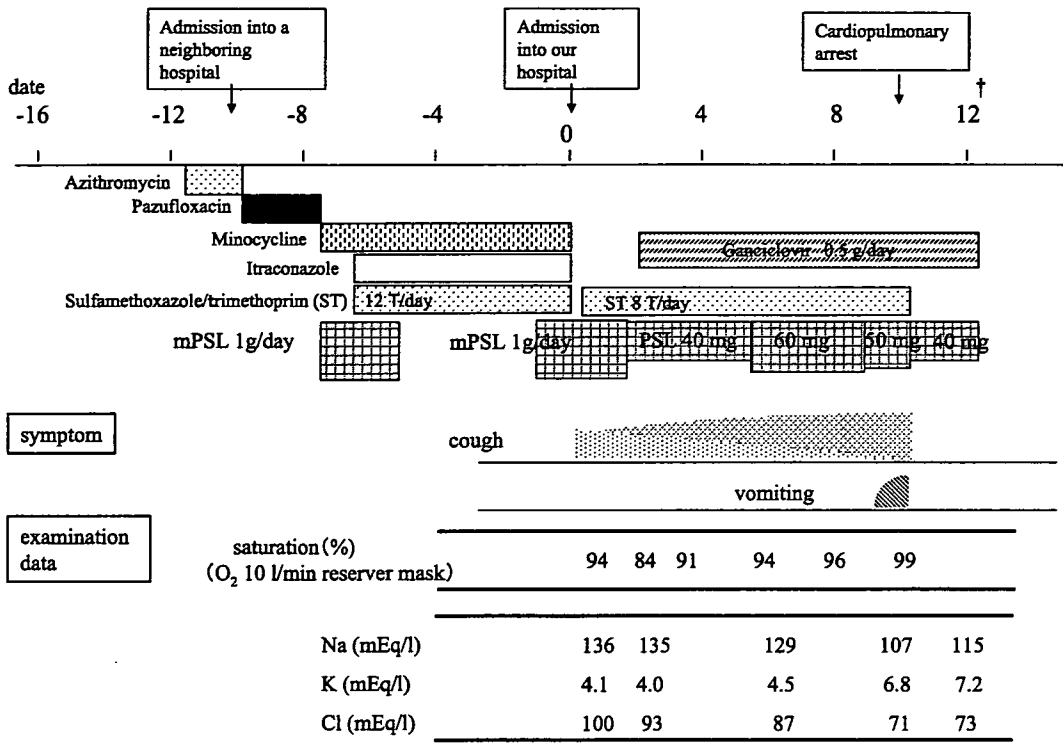

Figure 1. The clinical course of this case.

minemia, and high level of lactate dehydrogenase, C-reactive protein, and plasma β-D-glucan. The CD4-positive cell count was 13/μl, and the HIV-RNA loads were 1.1×10^5 copies/ml. The CMV antigenemia testing was positive (C7-HRP 60/150000 of WBC cells). Arterial blood gas analysis under 10 l/min oxygen inhalation (reserver mask) showed PaO_2 of 71 Torr and $PaCO_2$ of 31.3 Torr (Table 1). Chest radiography showed a diffuse interstitial infiltrate with ground glass appearance.

We diagnosed him as having pneumocystis pneumonia and CMV infection. The treatment for pneumocystis pneumonia with 8 tablets of sulfamethoxazole (3.2 g)/trimethoprim (640 mg) and 1 g of methylprednisolone (mPSL) was continued. In addition, administration of intravenous gancyclovir for CMV infection was started on the 2 nd day. His percutaneous oxygen saturation gradually improved, we reduced the amount of steroids to 40 mg of prednisolone on the 3rd day. However, he continued to complain of cough and dyspnea, so we added prednisolone (60 mg) on the 5th day, tapered to 50 mg on the 6th day, and to 40 mg on the 10th day. He has also complained of vomiting since the 9th hospitalization day.

On the 10th day, he suddenly fell into cardiopulmonary arrest. The laboratory tests one hour before the cardiopulmonary arrest showed serum sodium level of 107 mEq/l, chloride level of 71 mEq/l, and serum potassium level of 6.8 mEq/l (Table 2). Despite resuscitation, he died on the 12th day of admission (Fig. 1). Autopsy examination was performed 12 hours later. The weight of the right and left adrenal glands was 15 g and 10 g, respectively. An extensive hemorrhagic necrosis was macroscopically observed in both adrenal glands (Fig. 2a). Microscopic examination revealed diffuse hemorrhage and necrosis with intranuclear inclusion bodies in the bilateral adrenal glands (Fig. 2b, c). These findings were compatible with CMV-induced adrenal insufficiency. Diffuse alveolar damage and pulmonary hemorrhage were noticed in the bilateral lungs. Intranuclear inclusion bodies and cysts of *Pneumocystis jiroveci* were found in the lesions.

Discussion

The direct cause of death in this patient was considered to be mortal arrhythmia with hyperpotassemia due to CMV-associated adrenal insufficiency, which was diagnosed by his clinical features and post-mortem extermination. The differential diagnoses of electrolyte imbalance included acute renal failure, gastrointestinal losses, syndrome of inappropriate secretion of ADH (SIADH), and drug-induced. Acute renal failure was excluded because his serum creatinine level was in the normal range, and gastrointestinal losses were also excluded because there was no diarrhea. Agarwal et al reported that 36 of 103 patients (35%) with AIDS who were admitted for acute opportunistic infections had serum sodium of 130 mEq/l or less, and 23 patients had concomitant SIADH (1). Nevertheless, we could not deny SIADH because we checked neither ADH nor the urine electrolytes. Regarding the drug-induced electrolyte imbalance, Bevilacqua et al reported that a high dose of trimethoprim acted as an amiloride-like drug and induced a clinical state characterized by hyponatremia and hyperkalemia which is indistinguishable from hyporeninemic hypoaldosteronism (2). We

DOI: 10.2169/internalmedicine.46.1886

Table 1. Laboratory Data on Admission

【Peripheral blood】		
RBC	369	×10⁴/μl
Hb	11.0	g/dl
WBC	5400	/μl
lym	9.0	%
PLT	23.9	×10⁴/μl
【Biochemistry】		
TP	5.7	g/dl
Alb	2.6	g/dl
GOT	40	IU/l
GPT	20	IU/l
LDH	780	IU/l
ALP	180	IU/l
γ-GTP	29	IU/l
Na	136	mEq/l
K	4.1	mEq/l
Cl	100	mEq/l
Ca	8.1	mg/dl
BUN	10	mg/dl
Cre	0.6	mg/dl
【Serology/Immunology】		
β-D-glucan	69.6	pg/ml
CRP	13.1	mg/dl
CD4⁺	13	/μl
【Infection tests】		
HIV-RNA	110000	copies/ml
Cryptococcus Ag	(-)	
Aspergillus Ag	0.1	
CMV Ag	(+) (60/150000)	
【Artery blood gas analysis (10 l/min mask)】		
PO2	71	Torr
PCO2	31.3	Torr
pH	7.452	

Table 2. Laboratory Data at One Hour before the Cardiopulmonary Arrest Occurred

【Peripheral blood】		
RBC	389	×10⁴/μl
Hb	15.1	g/dl
WBC	3800	/μl
lym	4.0	%
PLT	19.2	×10⁴/μl
【Biochemistry】		
TP	7.8	g/dl
Alb	4.0	g/dl
GOT	24	IU/l
GPT	30	IU/l
LDH	374	IU/l
ALP	365	IU/l
γ-GTP	53	IU/l
BUN	28	mg/dl
Cre	0.8	mg/dl
Na	107	mEq/l
K	6.8	mEq/l
Cl	71	mEq/l
Ca	9.3	mg/dl

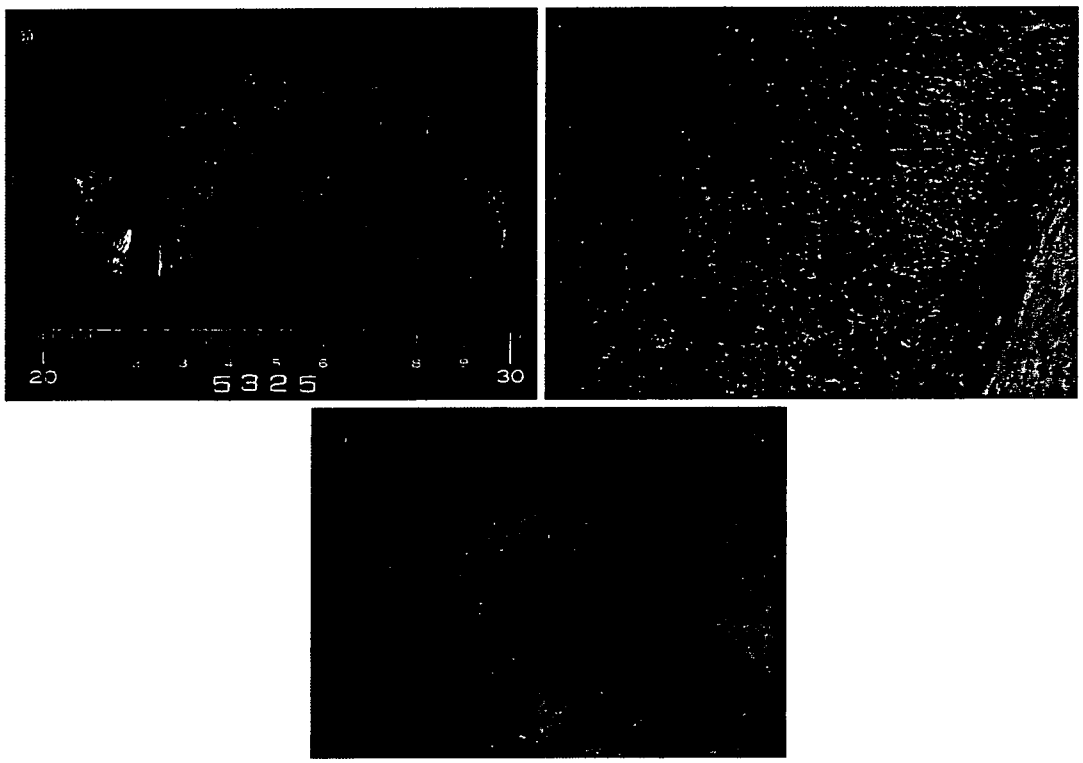

Figure 2. Autopsy examination of the adrenal glands revealed an extensive hemorrhage and necrosis with intranuclear inclusion bodies. (HE stain)

could not deny the influence of the drug-induced electrolyte imbalance, either.

CMV infection is a common opportunistic infection among the patients with advanced HIV disease. CMV infection can take many forms, including retinitis, colitis, esophagitis, encephalomyelitis, and other syndromes. Adrenal infection by CMV is a common autopsy finding in patients with AIDS (3). Pulakhandam *et al* reported that the incidence of adrenal involvement in 37 AIDS patients with CMV infection was 84% in their autopsy study (4). Grinspoon *et al* detected CMV in the adrenal glands of 33% to 88% of patients who died of AIDS (5). On the other hand, adrenal involvement by other pathogens is relatively rare (6). However, the clinical features of acute adrenal insufficiency are rare in AIDS patients with CMV infection. To our knowledge, there is the only one case report on CMV-induced adrenal insufficiency in a Japanese patient with AIDS (7). This is because glandular destruction does not typically exceed more than 50% of the adrenal tissue in most cases with CMV-induced adrenalitis (8). Because extensive adrenal hemorrhagic necrosis associated with CMV was observed in our post-mortem extermination, our patient was considered to have acute adrenal insufficiency.

The grave adrenal insufficiency was probably caused by

the delay of therapy for CMV and the treatment of pneumocystis pneumonia with steroid in our case. Adrenal insufficiency rarely develops in patients receiving supraphysiological doses of steroid for concomitant illness (9, 10). Razzaq *et al* first reported the development of CMV-induced adrenal failure in a patient with AIDS while receiving corticosteroid therapy. They reported that their patient had no manifestations related to his adrenal insufficiency which only became apparent on routine blood testing (11). They noticed a decrease in the serum sodium level, and doubted the occurrence of adrenal insufficiency. In the present case, vomiting was the only symptom that might have been related to adrenal insufficiency, and it occurred one day before cardiopulmonary arrest. Methylprednisolone and prednisolone, which were administered to our patient, have a weaker mineralocorticoid effect than glucocorticoid effect. Therefore, various manifestations associated with the glucocorticoid effect became unclear, and we did not notice his adrenal insufficiency until his serum electrolytes became deranged. The differential diagnoses of adrenal insufficiency in immunocompromised patients include viral, fungal, and mycobacterial diseases (12). Nonetheless, in our autopsy study, we found neither viral, fungal, nor mycobacterial infection except for CMV and *pneumocystis jirovecii* infection.

Some reports state that CMV-induced adrenal insufficiency improved with early appropriate treatment (6, 7). The electrolyte imbalance, which suggested the adrenal insufficiency, began on the 6th day of admission in our hospital. If we noticed this abnormality early, we could have saved his life. So, it is very important to pay careful attention to the manifestations of adrenal insufficiency in AIDS patients with CMV infection while receiving steroid therapy.

References

1. Agarwal A, Soni A, Ciechanowsky M, Chander P, Treser G. Hyponatremia in patients with the acquired immunodeficiency syndrome. Nephron **53**: 317-321, 1989.
2. Bevilacqua M. Hyponatremia in AIDS. Baillieres Endocrinol Metab **8**: 837-848, 1994.
3. Drew WL. Cytomegalovirus infection in patients with AIDS. J Infect Dis **158**: 449-456, 1988.
4. Pulakhandam U, Dincsoy HP. Cytomegaloviral adrenalitis and adrenal insufficiency in AIDS. Am J Clin Pathol **93**: 651-656, 1990.
5. Grinspoon SK, Bilezikian JP. HIV disease and the endocrine system. N Engl J Med **327**: 1360-1365, 1992.
6. Sanhes L, Michez E, Essig M, Rondeau E, Sraer JD. Successful treatment of CMV-induced adrenal insufficiency by gancyclovir in a patient with the acquired immunodeficiency syndrome. Nephrol Dial Transplant **10**: 704-705, 1995.
7. Fujii K, Morimoto I, Wake A, et al. Adrenal insufficiency in a patient with acquired immunodeficiency syndrome. Endocr J **41**: 13-18, 1994.
8. Glasgow BJ, Steinsapir KD, Anders K, Layfield LJ. Adrenal pathology in the acquired immune deficiency syndrome. Am J Clin Pathol **84**: 594-597, 1985.
9. Jacobs TP, Whitlock RT, Edsall J, Holub DA. Addisonian crisis while taking high-dose glucocorticoids: an unusual presentation of primary adrenal failure in two patients with underlying inflammatory disease. JAMA **260**: 2082-2084, 1988.
10. Cronin CC, Callaghan N, Kearney PJ, Murnaghan DJ, Shanaghan F. Addison's disease in patients treated with glucocorticoid therapy. Arch Intern Med **157**: 456-458, 1997.
11. Razzaq F, Dunbar EM, Bonington A. The development of cytomegalovirus-induced adrenal failure in a patient with AIDS while receiving corticosteroid therapy. HIV Med **3**: 212-214, 2002.
12. Guenthner EE, Rabinowe SL, Van Niel A, Naftilan A, Dluhy RG. Primary Addison's disease in a patient with the acquired immunodeficiency syndrome. Ann Intern Med **100**: 847-848, 1984.

© 2007 The Japanese Society of Internal Medicine
http://www.naika.or.jp/imindex.html